scientific reports

Check for updates

OPEN

Protective effects of indole-3-propionic acid against TCP-induced hearing loss in mice by mitigating oxidative stress and promoting neutrophil recruitment

Shuangshuang Mao[1,3], Zirui Zhang[1,3], Mao Huang[1,2,3], Ziying Zhang[1], Yu Hong[1], Xiaohua Tan[1], Fei Gui[1], Yifei Cao[1]✉, Fuzhi Lian[1]✉ & Rong Chen[1]✉

Sensorineural hearing loss (SNHL) poses a significant global health challenge with substantial socioeconomic and medical implications. The pathophysiology involves excessive reactive oxygen species (ROS) in the cochlea, inflammation, cellular apoptosis, etc. Tryptophan metabolite indole-3-propionic Acid (IPA), produced by gut microbiota, may offer therapeutic benefits by modulating inflammation, oxidative stress, and immune responses. However, the roles of IPA in protecting from treatment hearing loss in adult mice remain to be investigated. We previously validated that exposure to pesticide metabolite 3, 5, 6-Trichloro-2-pyridinol (TCP) caused hearing loss in mice. Herein, continuous administration of 40 mg/kg IPA for 21 days significantly attenuated the hearing threshold elevation in C57BL/6 mice exposed to 50 mg/kg TCP. IPA treatment reduced the loss of hair cells (HCs) and spiral ganglion neurons (SGNs), preserved nerve fibers, and reversed the damage to spiral ligaments (SL) and stria vascularis (SV). Similarly, IPA cotreatment decreased ROS accumulation in the cochlea and inhibited HC and SGN apoptosis. Transcriptomic analysis showed that IPA enhanced immune responses, particularly through neutrophil recruitment and the activation of regenerative signals like IFNγ. These findings underscore IPA's protective effects against TCP-induced hearing loss, highlighting the role of immune mechanisms in cochlear protection.

More than 430 million people worldwide suffer from disabling hearing loss, of which sensorineural hearing loss (SNHL) is the most common type. SNHL poses a significant global health challenge, impacting both the economy and the psychological well-being of affected individuals and their families[1]. SNHL is characterized by elevated hearing thresholds, often accompanied by a reduction in cochlear hair cells (HCs), thinning of the stria vascularis (SV), or loss of spiral ganglion neurons (SGNs)[2,3]. SNHL can result from various factors including genetic disorders, noise exposure, ototoxic medications, aging, and environmental toxins. These factors often have a cumulative effect, increasing the risk of developing SNHL[4]. Until now, only sodium thiosulfate has been approved in the United States for the prevention of cisplatin-induced hearing loss in children[5]. Available options such as hearing aids and cochlear implants provide varying degrees of benefit, but individual responses can differ significantly[6,7]. While gene therapy and stem cell therapy offer the potential for restoring HC function, their safety and ethical considerations are still under evaluation[8,9]. Although many natural products show promise in preclinical studies for treating SNHL, they have not been validated in clinical trials[10]. Therefore, the development of safe and effective drugs to prevent or treat hearing loss remains a critical area of research.

Intestinal microbes and their metabolites play great roles in regulating endocrine functions, neural signaling, energy metabolism, and the host's immune system, thereby maintaining intestinal and systemic homeostasis[11,12]. Indole-3-propionic acid (IPA) is one of the most abundant tryptophan metabolites in the human gut[13]. It has been shown that IPA can effectively ameliorate metabolic diseases such as nonalcoholic fatty liver disease, type 2 diabetes, obesity, and cardiovascular diseases[14]. IPA offers protective benefits by modulating inflammatory response, alleviating oxidative stress, reducing DNA damage, influencing lipid metabolism, and even stimulating the immune function of the host[12,15,16]. IPA regulates the inflammatory response in different

[1]School of Public Health, Hangzhou Normal University, Hangzhou 311121, Zhejiang, China. [2]Ji'an County People's Hospital, Jiangxi 343100, China. [3]These authors contributed equally: Shuangshuang Mao, Zirui Zhang and Mao Huang. ✉email: yfcao2007@163.com; fuzhi.lian@hznu.edu.cn; rongchen1984@hznu.edu.cn

cells through multiple pathways, a property that has been shown to be protective against several diseases. In lipopolysaccharides (LPS)-induced human astrocytes, IPA treatment prevented the increase in MCP-1, IL-12, IL-13, and TNF-α levels, thereby alleviating LPS-induced neurological inflammation[17]. Furthermore, IPA inhibited the Signal Transducer and Activator of Transcription 3 (STAT3) pathway in rat proximal tubular cells (HK-2). This action suppressed indoxyl sulfate-induced inflammation and fibrosis in these cells[18]. In addition, IPA acts as an antioxidant by scavenging free radicals and decreasing ROS levels[19]. IPA also reduced the level of DNA damage marker 8-hydroxy-2'-deoxyguanosine (8-OHdG), and inhibited the activities of apoptosis-related proteins such as caspase-9 and caspase-3, thus protecting against DNA damage and cell apoptosis induced by chlorpyrifos (CPF) in rat cerebellar and cerebral neurons[20]. Given these protective effects, further exploration of IPA's potential in safeguarding against SNHL and elucidating its underlying molecular mechanisms is essential.

3, 5, 6-Trichloro-2-pyridinol (TCP) is the metabolite of organophosphorus pesticide chlorpyrifos. Previous studies verified that both TCP and chlorpyrifos exhibit ototoxicity, leading to sensorineural hearing loss (SNHL)[21–23]. In C57BL/6 mice, exposure to TCP for 21 days caused an elevation of hearing thresholds, the loss of outer hair cells (OHCs) and SGNs, and the impairment of SV and spiral ligament (SL). TCP also leads to excessive ROS generation in House Ear Institute-Organ of Corti 1 (HEI-OC1) cells which are derived from the Corti organ of mouse and are considered to be an in vitro system for screening ototoxic drugs[21,22,24]. In this study, we used TCP-induced ototoxic model of C57BL/6 mice to assess the roles of IPA in mitigating cochlear damage. We employed various techniques, including RNA sequencing (RNA-seq) and differential expression analysis (DEG), to investigate the molecular mechanisms underlying the protective effects of IPA.

Results

IPA protects against TCP-induced hearing loss

To investigate whether IPA could reverse or functionally repair TCP-induced SNHL, adult male C57BL/6 mice were gavaged with IPA (20 and 40 mg/kg) and TCP (50 mg/kg) for 21 days (Fig. 1A). The ABR thresholds of the mice (day −7) were normal across all groups. After 21 days of administration, we performed a cross-sectional analysis of the ABR in each group (Fig. 1B). No difference in the ABR threshold between control and the 40 mg/kg IPA group was found at all tested frequencies (Click). 50 mg/kg TCP treatment alone significantly elevated the threshold at click (TCP vs. control: 40.00 ± 5.78 dB vs. 22.50 ± 4.08 dB, $p < 0.001$), co-treatment with 40 mg/kg TCP significantly decreased the TCP-elevated threshold (IPA + TCP vs. TCP: 27.38 ± 6.65 dB vs. 40.00 ± 5.78 dB, $p < 0.001$). Although no significant reduction was observed between 20 mg/kg IPA + TCP group and TCP group or between 40 mg/kg IPA + TCP group and 20 mg/kg IPA + TCP group, a dose-dependent trend of improvement in threshold by IPA was observed (Fig. 1C). Then 8-, 16-, and 32-kHz pure-tone burst stimuli were presented to mice. The results also revealed a significant reduction in the threshold for the 40 mg/kg IPA + 50 mg/kg TCP group compared with the TCP group (Fig. 1D). Altogether, 40 mg/kg IPA alleviated hearing loss induced by TCP exposure.

IPA reduces TCP-induced morphological damage of the cochlea

Histopathological analysis of cochlear sections was conducted (Fig. 2A). In the control group, there was a single row of inner hair cells (IHCs) and three rows of OHCs situated above the SCs, with no differences in morphology compared with the 40 mg/kg IPA group (Fig. 2A). In contrast, the organ of Corti in the 50 mg/kg TCP group showed a flat epithelium with loss of SCs (Fig. 2A, white asterisks). Notably, SCs remained intact in the 20 or 40 mg/kg IPA + 50 mg/kg TCP groups (Fig. 2A, white asterisks), suggesting a protective effect of IPA against TCP-induced damage in SCs. In the control group, SGNs were large, round, and ovoid-shaped (Fig. 2A). TCP exposure resulted in severe neurodegeneration of SGNs, whose nuclei appeared crumpled and deformed (Fig. 2A, yellow arrow). The number of SGNs was 48.00 ± 2.00 per 1000 μm^2 in the control group, showing no difference with the 40 mg/kg IPA group. However, the number of SGNs decreased to 29.40 ± 2.61 per 1000 μm^2 in the TCP-exposed group (compared with control group, $p < 0.001$), whereas that in the 20 or 40 mg/kg IPA + 50 mg/kg TCP groups were reversed to 36.25 ± 2.06 (compared with TCP group, $p < 0.01$), and 45.00 ± 2.45 per 1000 um^2 ($p < 0.0001$), respectively (Fig. 2C). These findings suggest that IPA exerts protective effects on TCP-damaged SCs and SGNs in the mouse cochlea. The SV thickness was 27.62 ± 1.85 μm in the control group and 19.71 ± 0.44 μm in the 50 mg/kg TCP group, showing that TCP could cause damage to the SV ($p < 0.001$). In the 20 or 40 mg/kg IPA + 50 mg/kg TCP group, the SV thickness was 24.85 ± 1.78 μm and 27.58 ± 0.58 μm, respectively, significantly alleviating the thinning of the SV caused by TCP exposure ($p < 0.001$) (Fig. 2D). According to the structural schematic of cochlear sections, type I and V fibroblasts in the SL were present in the 40 mg/kg IPA group as in the control group. However, the 50 mg/kg TCP group exhibited loss of type I and V fibroblasts in the SL (Fig. 2A, B). These impairments were ameliorated in the IPA (20 mg/kg, 40 mg/kg) + TCP (50 mg/kg) group (Fig. 2A, B). These data indicate that IPA treatment can reverse TCP-induced damage to the SV and SL.

IPA protects against TCP-induced damage of HCs and SGNs

To obtain a more comprehensive view of HCs, SGNs, and NFs on the basement membrane, we used an HC-specific anti-myosin 7a antibody and the nuclear marker DAPI to label the HCs. Figure 3A illustrates the ordered arrangement of the IHCs and OHCs in the control group, with the OHCs stereocilia arranged in a normal V-shape. No difference was found in the number of HCs between the control group (49.6 ± 1.34 per 100 μm) and the 40 mg/kg IPA group (48.25 ± 1.89 per 100 μm), whereas the number of HCs in the TCP-exposed group decreased to 39.00 ± 2.35 per 100 μm (compared with control group, $p < 0.001$). The number of HCs in the 20 or 40 mg/kg IPA + 50 mg/kg TCP group was maintained at 42.50 ± 1.05 (compared with TCP group, $p < 0.05$), and 46.20 ± 3.42 per 100 μm (compared with TCP group, $p < 0.001$), respectively (Fig. 3B). The morphology of the SGNs was also examined. Representative confocal micrographs of SGNs and nerve fibers (NFs) were stained

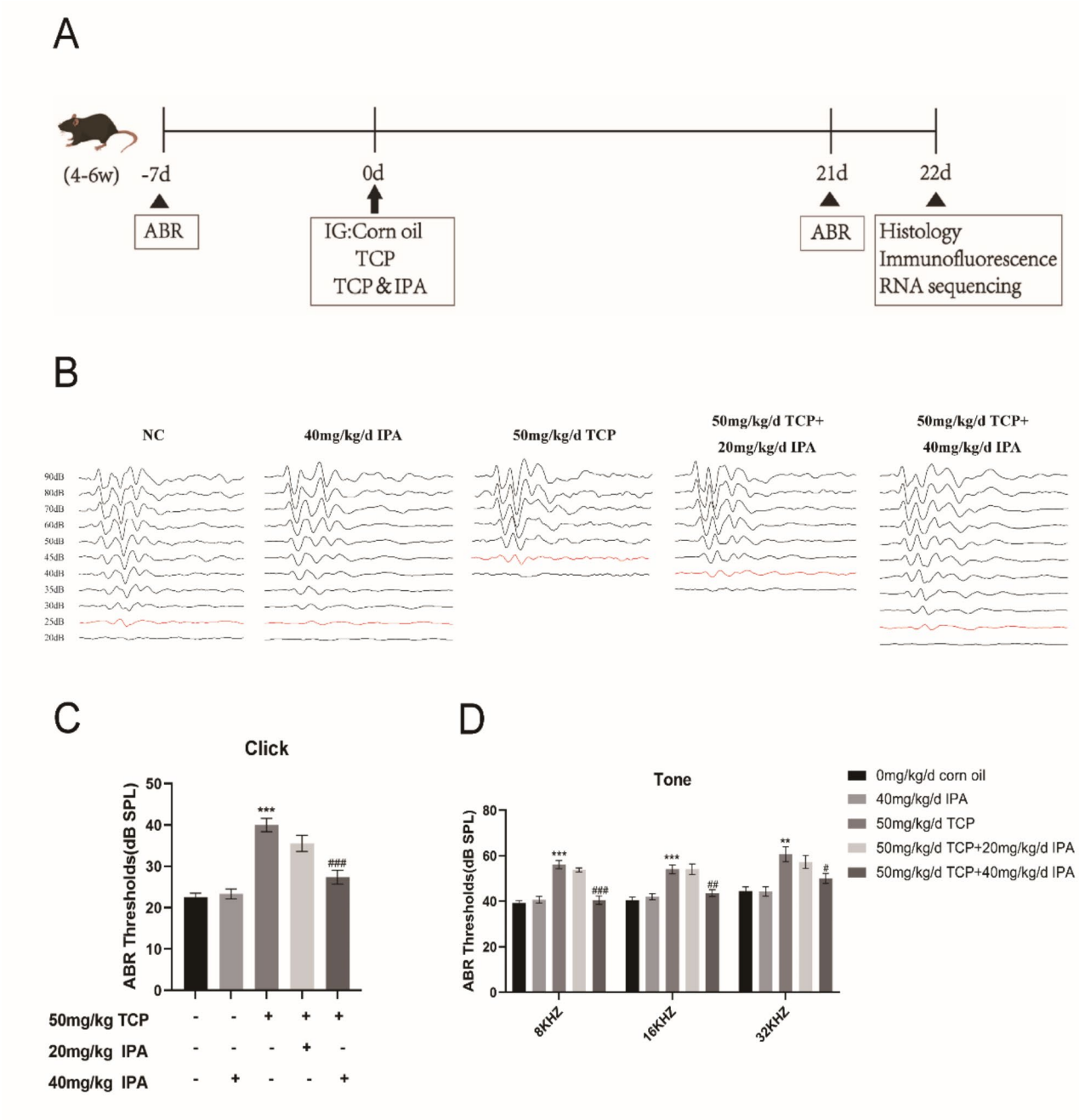

Fig. 1. IPA treatment reduced TCP-induced ABR threshold changes. (**A**) Schematic diagram of the experimental flow of the ABR test, (**B**) ABR test of the mice with different treatments, (**C**) ABR threshold plots at Click stimulation after 21 days of gavage in NC, 40 mg/kg IPA, 50 mg/kg TCP, 20 mg/kg IPA + 50 mg/kg TCP, and 40 mg/kg IPA + 50 mg/kg TCP groups, (**D**) ABR threshold plots at 8 kHz, 16 kHz, 32 kHz pure tone stimulation after 21 days of gavage in NC, 40 mg/kg IPA, 50 mg/kg TCP, 20 mg/kg IPA + 50 mg/kg TCP, and 40 mg/kg IPA + 50 mg/kg TCP groups. Data are represented the means ± SD, $n = 8$ for each group; **: $p < 0.01$ compared with control; ***: $p < 0.001$ compared with control; #: $p < 0.05$ compared with 50 mg/kg TCP group; ##: $p < 0.01$ compared with 50 mg/kg TCP group; ###: $p < 0.001$ compared with 50 mg/kg TCP group by one-way ANOVA with Bonferroni posthoc test.

with Tuj1, while the nuclei were labeled with DAPI. In the control group, SGNs had a large round nucleus (blue) located within the cytoplasm (red) (Fig. 4A). After TCP exposure, the number of SGNs decreased, and the remaining ones appeared smaller. The nuclei were pyknotic or undergoing karyorrhexis (Fig. 4A, white asterisks); however, SGNs in the TCP-exposed groups treated with 20 or 40 mg/kg IPA exhibited recovery in both number and morphology (Fig. 4A). TCP treatment also resulted in disordered, broken, or absent NFs. In

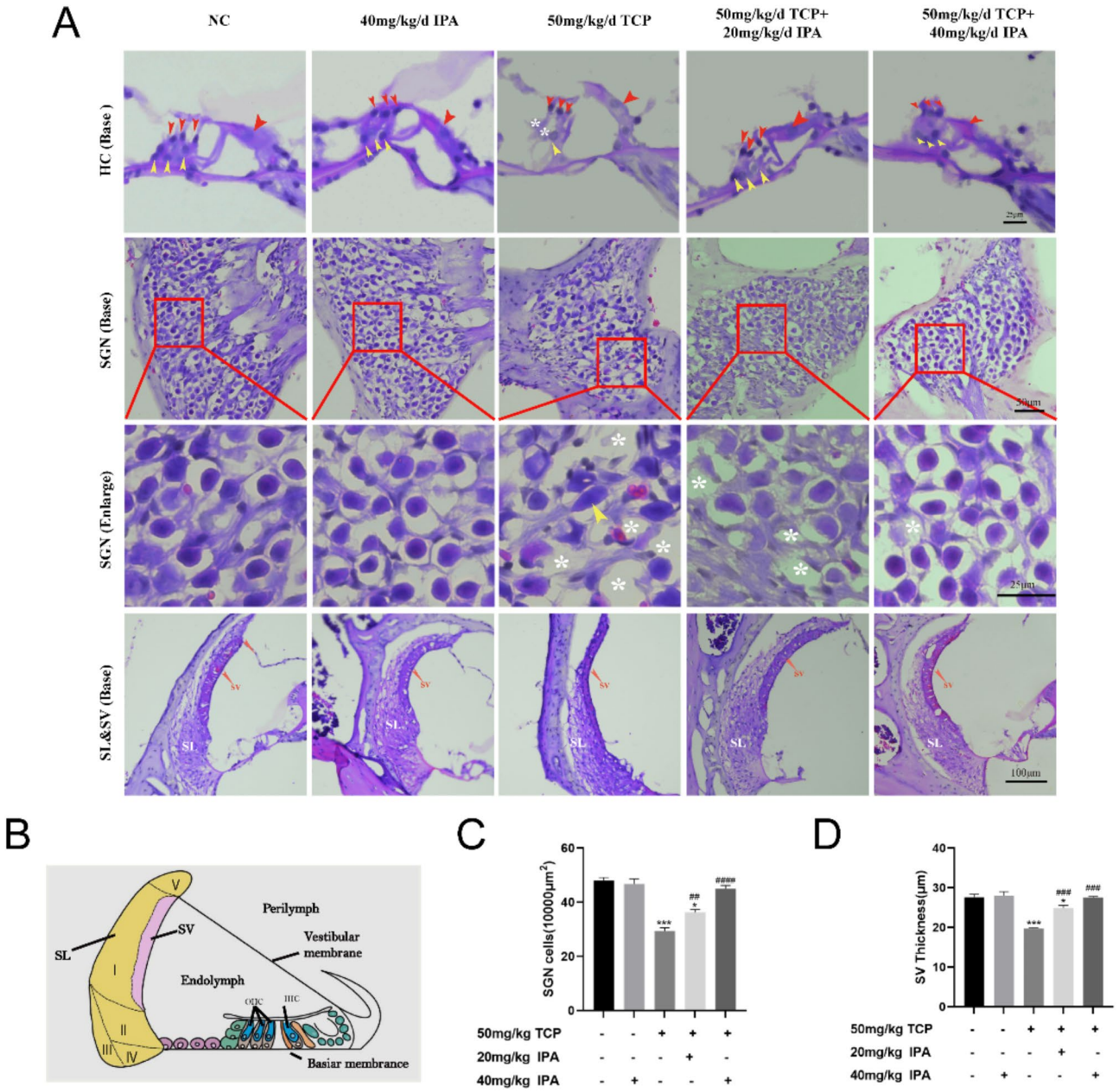

Fig. 2. IPA treatment reduced TCP-induced morphological damage of the cochlea. (**A**) H&E staining of HCs, SGNs, SV, SL in the basal turn of the cochlea after 21 days of gavage in corn oil, 40 mg/kg IPA, 50 mg/kg TCP, 20 mg/kg IPA + 50 mg/kg TCP, and 40 mg/kg IPA + 50 mg/kg TCP groups(corn oil as solvent, n = 3), (**B**) schematic structure of cochlea sections, (**C**) bar graph showing the average number of SGNs in the basal turn of the cochlea, (**D**) bar graph showing the average thickness of SV in the basal turn of the cochlea. Bar = 100 μm; Data represent the means ± SD; **: $p < 0.01$ compared with control; ***: $p < 0.001$ compared with control; #: $p < 0.05$ compared with 50 mg/kg TCP group; ##: $p < 0.01$ compared with 50 mg/kg TCP group; ###: $p < 0.001$ compared with 50 mg/kg TCP group; ####: $p < 0.0001$ compared with 50 mg/kg TCP group by one-way ANOVA with Bonferroni post hoc test.

contrast, IPA treatment led to partial recovery of the NFs (Fig. 4B). These findings demonstrate that IPA could protect against neurodegeneration induced by TCP exposure in the cochlea.

IPA reduces the levels of ROS induced by TCP exposure

Reactive oxygen species (ROS) and oxidative stress significantly contribute to cell death under stressful conditions. Previous studies have shown that TCP exposure increases ROS levels in the cochlea and leads to hearing loss[21]. Hence, DHE staining of tissue sections was performed, and the intensity of red fluorescence was analyzed. No significant differences in ROS levels were observed between the control and 40 mg/kg IPA groups. However, exposure to 50 mg/kg TCP resulted in an increase in ROS in SGNs, HCs, and SV (Fig. 5). In contrast,

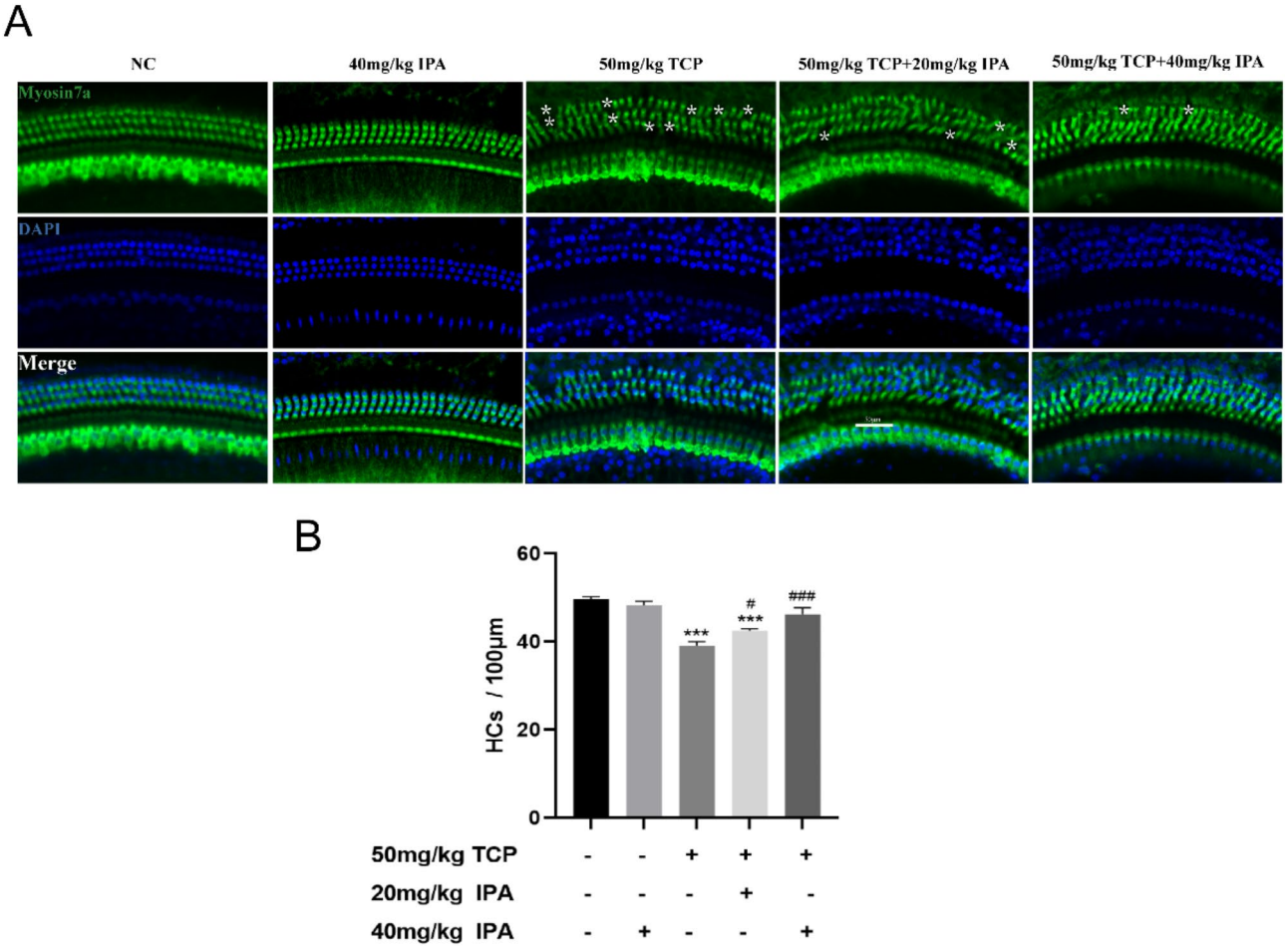

Fig. 3. IPA treatment protected against TCP-induced damage of HCs. (**A**) Representative figures of HCs in the basal turn of mice cochlea after 21 days of gavage in NC, 40 mg/kg IPA, 50 mg/kg TCP, 20 mg/kg IPA + 50 mg/kg TCP, and 40 mg/kg IPA + 50 mg/kg TCP groups (corn oil as solvent), (**B**) Bar graph showing the average number of HCs in basal turn after 21 days of gavage in NC, 40 mg/kg IPA, 50 mg/kg TCP, 20 mg/kg IPA + 50 mg/kg TCP, and 40 mg/kg IPA + 50 mg/kg TCP groups (corn oil as solvent, n=3). Data represent the mean ± SD; ***: $p < 0.001$ compared with control; #: $p < 0.05$ compared with 50 mg/kg TCP group; ###: $p < 0.001$ compared with 50 mg/kg TCP group by one-way ANOVA with Bonferroni post hoc test.

ROS fluorescence was reduced in the 20 mg/kg or 40 mg/kg IPA + 50 mg/kg TCP groups, and the 40 mg/kg IPA + 50 mg/kg TCP groups showed the weakest fluorescence intensity, which was close to that of the control group (Fig. 5). IPA treatment effectively counteracts the cochlear redox imbalance caused by TCP exposure.

IPA reduces TCP-induced apoptosis in HCs and SGNs

Apoptosis is a major mode of cell death in response to TCP exposure in HEI-OC1 cells and adult mice[22,23]. Hence, we performed immunofluorescence staining. Few TUNEL-positive cells were detected in the control and 40 mg/kg IPA groups (Fig. 6A, B). By contrast, TCP treatment significantly increased the proportion of TUNEL-positive cells (Fig. 6A, B, white arrows;). Specifically, TCP exposure led to a significant increase to the proportion of TUNEL-positive cells in OHCs (9.77% ± 1.75%, $p < 0.0001$) and SGNs (10.04% ± 2.26%, $p < 0.001$) (Fig. 6C, D). However, the proportion of TUNEL-positive cells in HCs and SGNs were decreased to 5.18% ± 1.75% ($p < 0.001$) and 2.91% ± 2.94% ($p < 0.01$) in the 20 mg/kg IPA + 50 mg/kg TCP group compared to those in the TCP only group. An even more decrease of TUNEL-positive cells in HCs (0.57% ± 1.14%, $p < 0.0001$) and SGNs (0.79% ± 1.38%, $p < 0.001$) was observed in the 40 mg/kg IPA + 50 mg/kg TCP group (Fig. 6C,D). These results suggest that IPA effectively inhibited TCP-induced apoptosis in HCs and SGNs.

IPA affects immune and inflammatory response

ROS play a crucial role in various signaling pathways related to immune cells, inflammatory factors, and inflammatory responses[25]. To further investigate the mechanism, RNA sequencing was performed on mouse cochlea in the control, 50 mg/kg TCP, and 40 mg/kg IPA + 50 mg/kg TCP groups. Principal component Analysis (PCA) revealed that PC1 explained 65.34% of the variation, while PC2 accounted for 20.17%. The PCA showed a clear separation into three groups with a significance of 0.01 (Fig. 7A). Cluster analysis of the heatmap showed

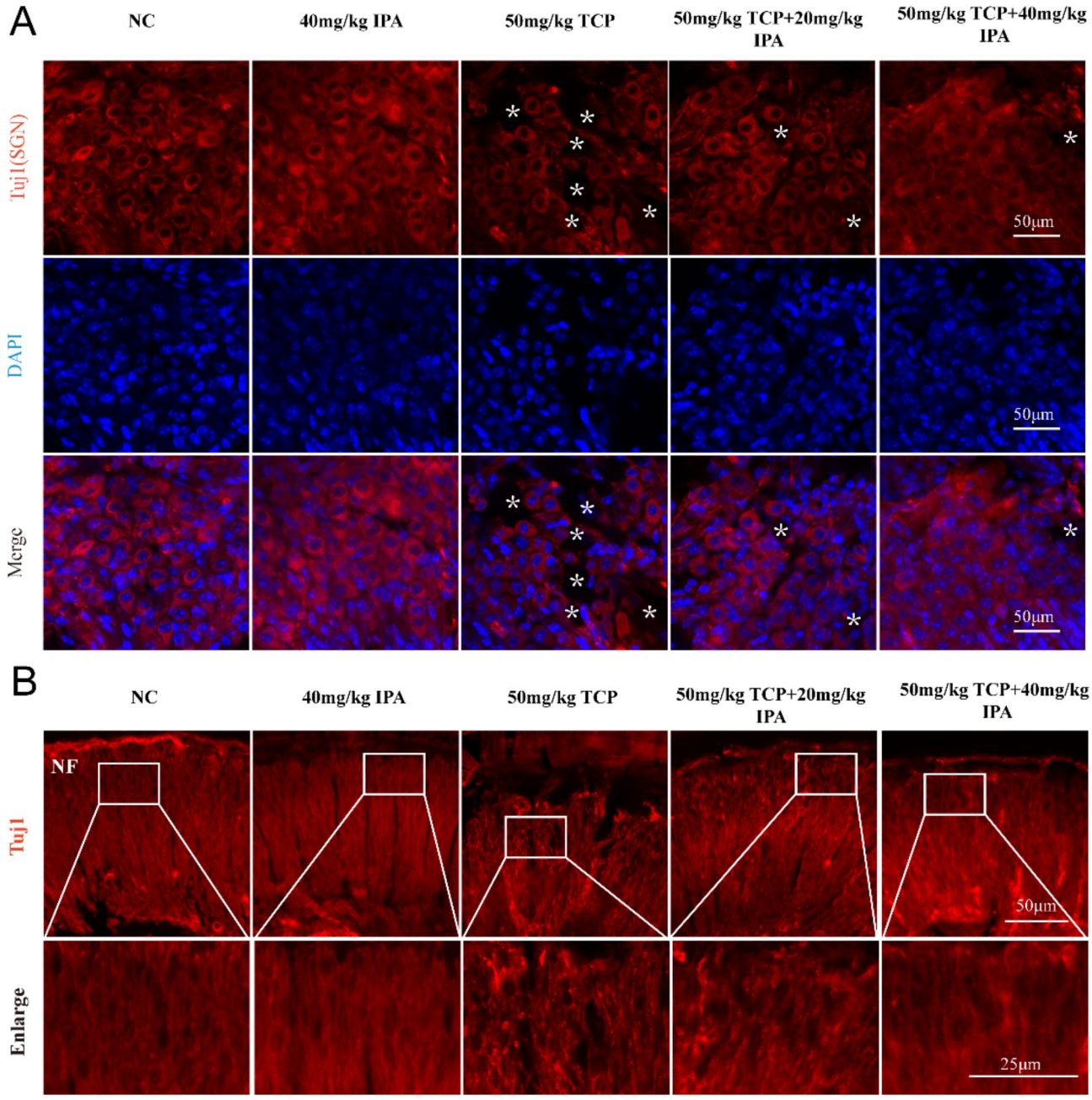

Fig. 4. IPA treatment protected against TCP-induced neurodegeneration. (**A**) Morphological results of SGNs in the basal turn of mouse cochlea after 21 days of gavage in the NC, 40 mg/kg IPA, 50 mg/kg TCP, 20 mg/kg IPA + 50 mg/kg TCP, and 40 mg/kg IPA + 50 mg/kg TCP groups (Corn oil as solvent, $n = 3$). Bar = 50 μm; (**B**) Morphological results of NFs in the basal turn of mice cochlea after 21 days of gavage in the NC, 40 mg/kg IPA, 50 mg/kg TCP, 20 mg/kg IPA + 50 mg/kg TCP, and 40 mg/kg IPA + 50 mg/kg TCP groups (Corn oil as solvent, $n = 3$). Bar = 50 μm and 25 μm.

that the biological replicates were consistently grouped, demonstrating a clear distinction between the groups and indicating the high reliability of the transcriptome data (Fig. 7B). Differentially expressed genes (DEGs) analysis revealed 1434 up-regulated and 773 down-regulated genes between the IPA + TCP and TCP groups (Supplemental file). Gene Ontology (GO) categories analysis revealed that the up-regulated genes in the IPA + TCP group were involved in various immune-related biological processes (BP), such as the immune system response, autoimmune response, and inflammatory response (Fig. 7C,D). Additionally, Kyoto Encyclopedia of Genes and Genomes (KEGG) analysis identified that these up-regulated genes participated in several immune and inflammatory response signaling pathways, such as cytokine-cytokine receptor interactions, cytokine and growth factor pathways, and the TNF signaling pathway (Fig. 7E,F). Besides, cytokines (TNF, IL-2ra, IL-2rg, and IL-12b), inflammasome components (NLRP3, PSTPIP1, and MEFR), inflammatory processes (MMP3,

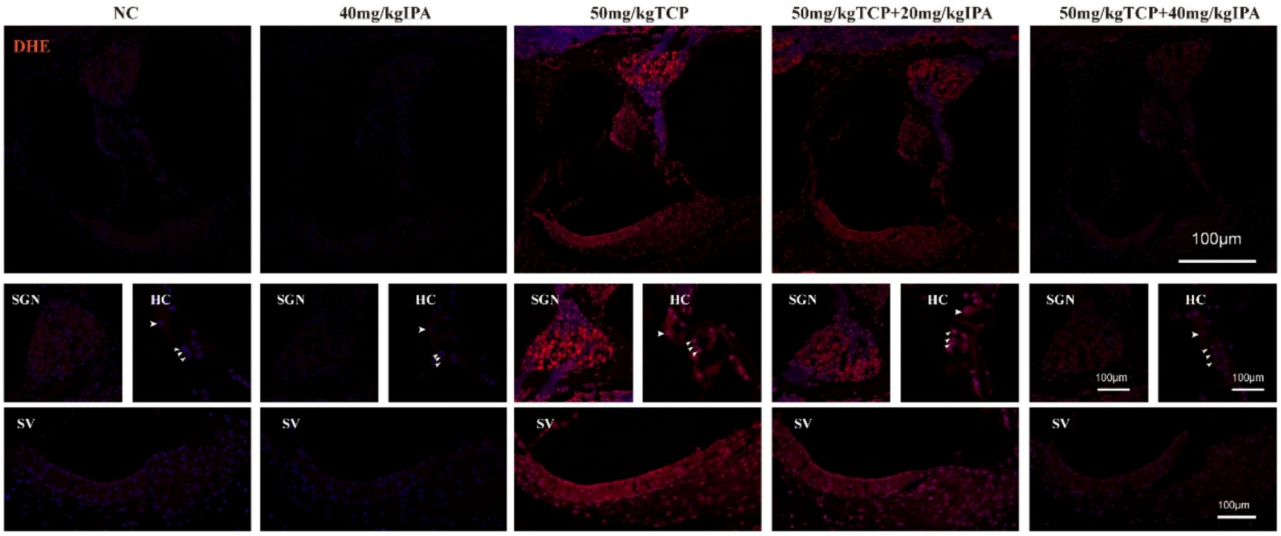

Fig. 5. Protective effects of IPA against oxidative stress included by TCP. DHE staining results of SGNs, HCs, and SV in basal turn after 21 days of gavage in the NC, 40 mg/kg IPA, 20 mg/kg IPA + 50 mg/kg TCP, and 40 mg/kg IPA + 50 mg/kg TCP groups (corn oil as a solvent, $n = 3$); Bar = 100 μm; Red fluorescence represents DHE staining; blue fluorescence represents DAPI staining.

MMP8, and MMP9), immune cell recruitment and IFNγ signaling (CCL8, GBP2, GBP3, H2-Q7, and NOS2) were significantly up-regulated (Fig. 8A).

IPA acts by promoting neutrophils recruitment

Serger et al. revealed that IPA promoted nerve regeneration and repair by neutrophils recruitment[16]. Neutrophils promote neuronal survival and axonal regeneration in a mouse model of optic nerve crush (ONC) injury[26]. Similarly, three hallmark genes-neutrophil ligand (Cd177), endothelial neutrophil chemoattractant chemokine (CXCL1) and a marker protein for neutrophil activation and chemotaxis (CXCR2) were significantly upregulated in the IPA + TCP group compared with TCP group (Fig. 8A). We performed immunofluorescence staining to detect the expression of a neutrophil-specific marker (Ly6G). The results showed that fluorescence signals of Ly6G were significantly decreased in the TCP-exposed group compared to the control and 40 mg/kg IPA groups. Importantly, the Ly6G fluorescence signals in the 40 mg/kg IPA + TCP group were significantly increased compared with the TCP group (Fig. 8B). This indicates that IPA effectively elevates neutrophil levels by recruiting neutrophils to the cochlea.

Discussion

IPA, a metabolite of tryptophan produced by the gut flora, is known for its benefits to gastrointestinal health, immune modulation, neuroprotection, and cardiovascular risk reduction[27]. In this study, we used a TCP-induced hearing loss model in C57BL/6 mice to demonstrate that IPA treatment effectively prevented TCP-induced SNHL. Specifically, IPA mitigated TCP-elevated hearing thresholds and preserved TCP-damaged cochlear morphology. Immunofluorescence staining revealed that IPA reduced ROS accumulation in the cochlea, thereby alleviating oxidative stress. Moreover, IPA treatment prevented apoptosis of HCs and SGNs, both of which are essential for hearing function. Transcriptome analysis showed significant neutrophil recruitment in the cochlea of the IPA + TCP group, along with an increase in IFNγ signaling. Thus, IPA, a prominent tryptophan metabolite, appears to be a promising agent for protecting against hearing loss.

Environmental toxins or noise exposure can lead to hearing loss by damaging or destroying SCs, HCs, and SGNs. Such damage is also associated with severe atrophy of fibroblasts, accompanied by thinning of the SV in mice. These changes result in a significant elevation of hearing thresholds, that was detected by ABR test[22,28]. Meanwhile, combined with immunohistological analysis allows for a comprehensive investigation of both cochlear and neural damage[29,30]. Mechanisms of hearing loss involve oxidative stress, excessive inflammation, and apoptosis, etc[23,31,32]. Elevated ROS levels can overwhelm the innate antioxidant defenses, leading to oxidative stress, lipid peroxidation, and protein damage, ultimately causing cellular dysfunction[25,33,34]. Previous findings suggested that TCP causes DNA damage and apoptosis in the cochlea by increasing ROS production and inhibiting the expression of antioxidant enzymes, thereby impairing hearing[21]. Tryptophan-derived indole metabolites have been proven to be antioxidants and free radical scavengers, while IPA is a deamination product of tryptophan. In this study, IPA effectively reduced ROS levels in the cochlea, as demonstrated by DHE staining, particularly in SGNs and HCs. Meanwhile, the elevated proportion of TUNEL-positive cells in HCs and SGNs was reversed in IPA-treated TCP-exposed mice. Owumi et al. reported the protective role of IPA against liver and kidney damage induced by chlorpyrifos (CPF). IPA effectively reduced excessive free radical generation through the mitigation of lipid peroxidation and oxidative stress. This, in turn, reversed the augmentation of ROS and

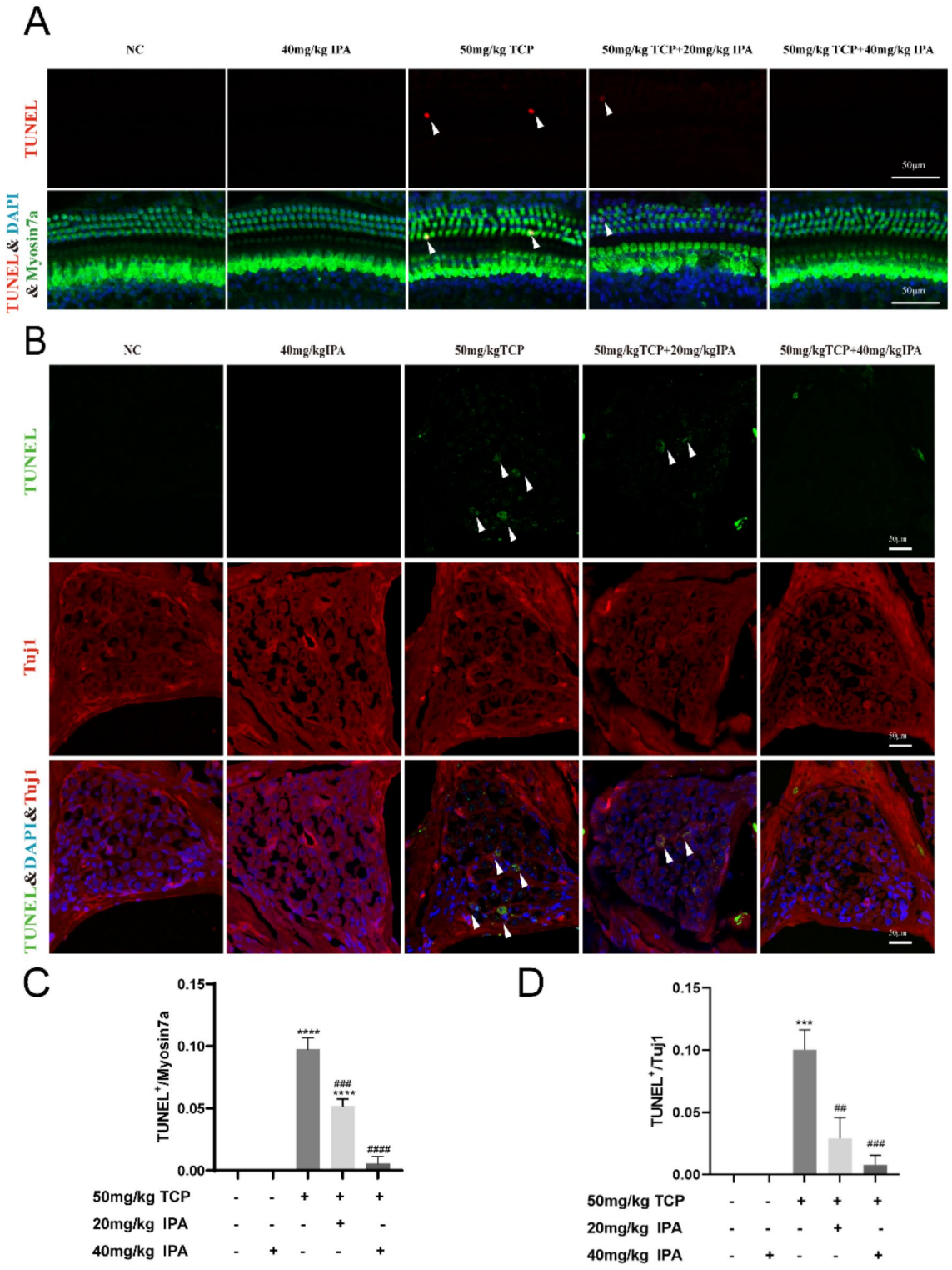

Fig. 6. IPA alleviated the apoptosis of HCs and SGNs induced by TCP. (**A**) TUNEL staining results of HCs in the basal turn of cochlear basilar membrane in the group of NC, 40 mg/kg IPA, 50 mg/kg TCP, 20 mg/kg IPA + 50 mg/kg TCP, and 40 mg/kg IPA + 50 mg/kg TCP after 21 days of gavage (corn oil was used as a solvent, $n = 3$), (**B**) TUNEL staining results of SGNs in the basal turn of the cochlear basilar membrane in the group of NC, 40 mg/kg IPA, 50 mg/kg TCP, 20 mg/kg IPA + 50 mg/kg TCP, and 40 mg/kg IPA + 50 mg/kg TCP after 21 days of gavage (corn oil was used as a solvent, $n = 3$), (**C**,**D**) Results of TUNEL-positive cell counts after 21 days of gavage in NC, 40 mg/kg IPA, 50 mg/kg TCP, 20 mg/kg IPA + 50 mg/kg TCP, and 40 mg/kg IPA + 50 mg/kg TCP groups (Corn oil as solvent, $n = 3$); Bar = 50 μm; Data expressed as a percentage; ***: $p < 0.001$ compared with control; ****: $p < 0.0001$ compared with control; ##: $p < 0.01$ compared with 50 mg/kg TCP group; ###: $p < 0.001$ compared with 50 mg/kg TCP group; ####: $p < 0.0001$ compared with 50 mg/kg TCP group by one-way ANOVA with Bonferroni post hoc test.

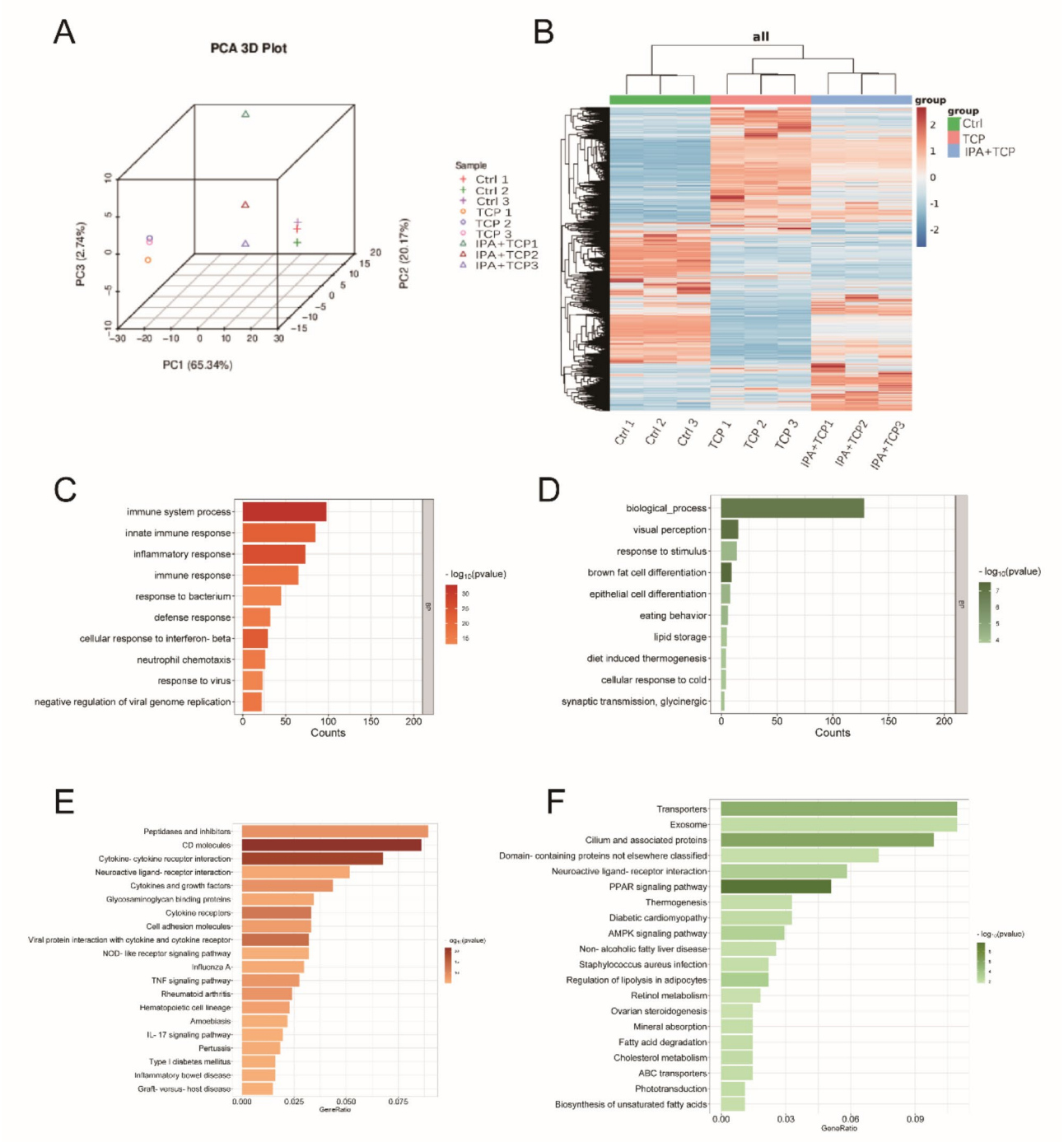

Fig. 7. Gene expression patterns in mice cochlea by RNA-Seq analysis. (**A**) Three-dimensional (3D) PCA plot showing loadings of PC1, PC2 and PC3, (**B**) Transcriptomic heatmap indicates gene expressive levels in three groups. (Red/orange colors represent highly expressed genes and blue colors represent down-expressed genes in three groups, (**C**) Up-regulated genes by GO enrichment analysis, (**D**) Down-regulated genes by GO enrichment analysis, (**E**) Up-regulated pathways for KEGG pathway analysis of DEGs, (**F**) Down-regulated pathways for KEGG pathway analysis of DEGs; PCA employs linear algebraic computational methods to perform dimensionality reduction and extract principal components from tens of thousands of gene variables; the StringTie software package (https://ccb.jhu.edu/software/stringtie/) is suitable for transcript assembly, quantification, and differential expression analysis of RNA - Seq data.

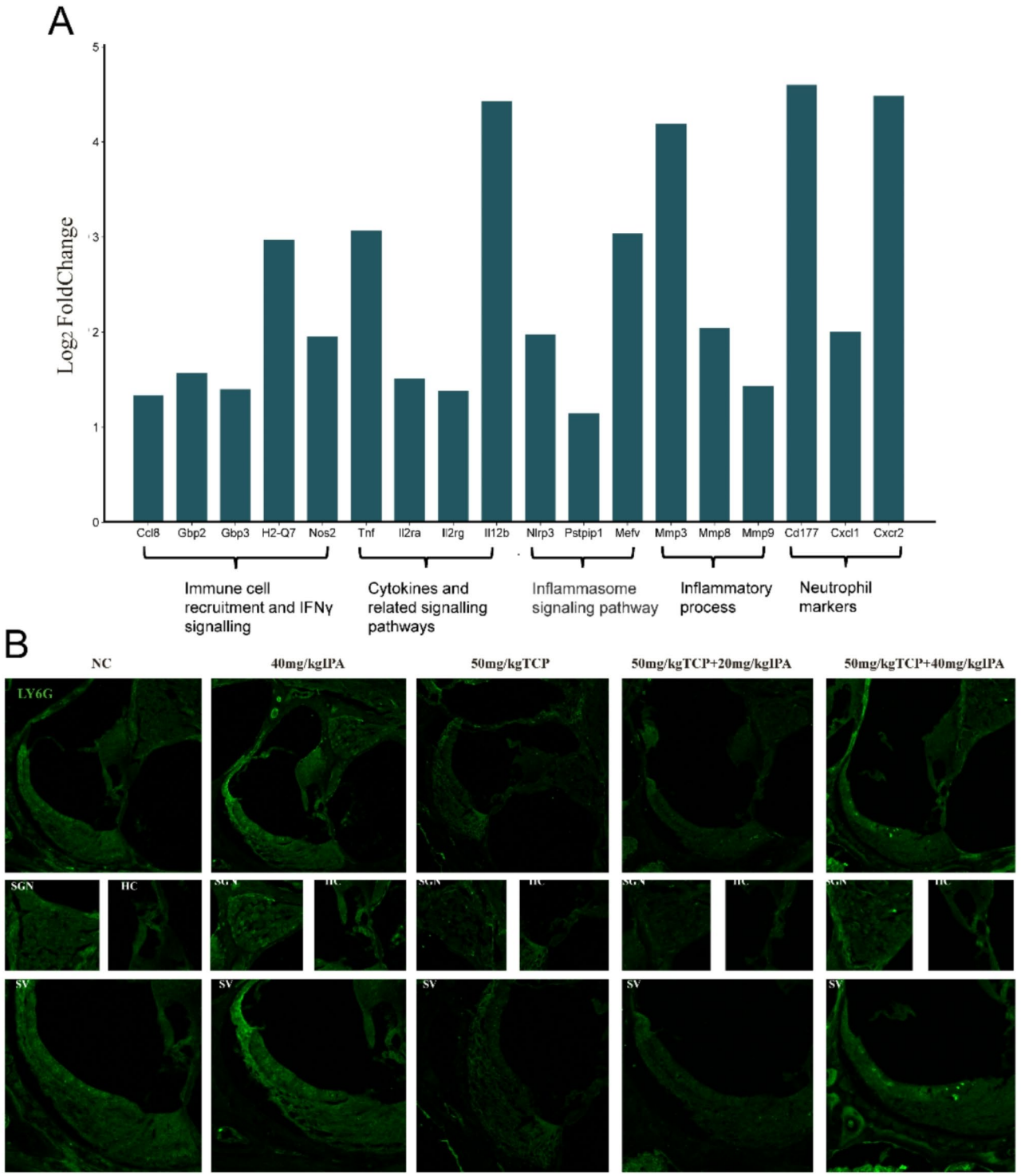

Fig. 8. IPA-dependent cochlear protection relies on neutrophil recruitment. (**A**) Comparison of gene expression related to the regulation of immune function and inflammatory response in the mouse cochlea between IPA + TCP and TCP group, (**B**) Ly6G immunostaining in cochlear sections of mice in the NC, 40 mg/kg IPA, 50 mg/kg TCP, 50 mg/kg TCP + 20 mg/kg IPA, and 50 mg/kg TCP + 40 mg/kg IPA groups after 21 days of gavage (Corn oil as solvent, $n = 3$); Bar = 50 μm.

lipid peroxides in the liver and kidney of rats co-exposed to CPF, mitigating the neurotoxic and behavioral abnormalities induced by CPF in rats[20]. Several natural products with antioxidant properties have been shown to prevent and treat SNHL by reducing ROS production and lowering oxidative stress[10]. For example, curcumin effectively attenuates HC apoptosis and cellular senescence thereby mitigating age-induced hearing loss[35];

Hesperetin potentially mitigates ototoxicity by boosting antioxidant enzymes, lowering oxidant parameters, and protecting against apoptosis resulting from a proliferation of cochlear cells[36].

On the other hand, recent studies reveal that IPA promotes nerve regeneration and repair through neutrophils recruitment and upregulated the IPA-dependent IFNγ signaling pathway in a mouse model of sciatic nerve crush (SNC)[16]. Wang et al. reported that neutrophil-produced cytokines synergistically promoted nerve regeneration by clearing nerve debris and inducing macrophages to become an anti-inflammatory phenotype of M2 in a rat model of sciatic injury[37]. Neutrophils promoted neuronal survival and axonal regeneration by secreting the growth factors in mouse model of optic nerve crush (ONC) injury[26]. These studies have shown that infiltration of neutrophils can promote the release of cytokines and growth factors, which play a positive role in tissue repair and neural function recovery. Transcriptome sequencing results gave hints on possible protective roles of IPA. In the IPA + TCP group, most enriched GO terms were directly related to biological processes and molecular functions of neutrophils and chemotaxis, such as "immune process", "inflammatory response", and "neutrophil chemotaxis". The KEGG pathway analysis revealed significant enrichment of DEGs in the "cytokine-cytokine receptor interaction" pathway. The expression levels of neutrophil ligand (Cd177), neutrophil chemokine (CXCL1) and the receptor of CXCL1 (CXCR2) were significantly upregulated in the IPA + TCP group. CXCL1 binds to its receptor, CXCR2, on neutrophils, activating them and initiating neutrophil chemotaxis[38]. Immunofluorescence analysis also confirmed increased infiltration of neutrophils in the IPA + TCP group. The release of pro-inflammatory cytokines initiates CXCL1 expression and neutrophil chemotaxis[38]. The inflammasome, which is responsible for the recruitment and activation of neutrophils, has been shown to trigger the release of numerous proinflammatory cytokines and chemokines[39,40]. Immune process-related genes, such as matrix metalloproteinases (MMPs), are known to influence neutrophil migration along chemotactic gradients and are involved in neutrophil infiltration[41]. The upregulation of these genes further give insight into the IPA-dependent mechanisms of neutrophil activation and infiltration in the cochlea.

Additionally, neutrophils releases immunomodulatory cytokines such as IFNγ during their recruitment to inflammation sites[42]. Emerging evidence suggests that IFNγ plays a role in neural repair processes. For example, acute IFNγ treatment increased the neurite length of human induced pluripotent stem cells (HIPSCs)[43]. Injured DRG axons released IFNγ, which promotes CNS axon regeneration through the cGAS-STING pathway[44]. Serger et al. verified that IPA enhanced the expression of IFNγ in the DRG neuronal cells of SNI model[16]. Our study got similar results. KEGG pathway analysis indicated significant enrichment of "cytokines and growth factors" and increased levels of IFNγ- signaling genes in the cochlea. This suggests that IPA may facilitate the recruitment of neutrophils to SGNs in the cochlea, which could work in tandem with downstream pathways involving cytokines like IFNγ. The synergistic action of neutrophil recruitment and IFNγ signaling likely underpins IPA's protective effects on cochlear structures, particularly SGNs. This immunomodulatory mechanism represents a novel aspect of IPA's otoprotective effects, distinguishing it from other antioxidant compounds.

Conclusions

This study investigates the protective effects of IPA on hearing against TCP-induced ototoxicity. IPA demonstrates significant potential in preventing TCP-induced hearing loss and associated cochlear damage through mechanisms such as reducing oxidative stress, inhibiting apoptosis, and modulating the immune response. It is noteworthy that IPA's protective effects involve the recruitment of neutrophil chemotaxis. However, the precise molecular mechanisms underlying the neuroprotective effects mediated by neutrophil chemotaxis need further exploration. In summary, IPA, a gut microbiota-derived tryptophan metabolite, shows promise as a novel therapeutic approach for preventing drug-induced ototoxicity.

Methods

Antibodies, reagents, and kits

Antibodies used in this study including Mouse anti-Tubulinβ3 antibody (Cat:801201, BioLegend, CA, US), Myosin7a antibody(Cat:25-6790, proteus biosciences, MA, US), and Ly6G antibody (Cat: BE0075-1, Bio X Cell, NH, US); Anti-Rabbit Alexa Fluor 488 (1:500 dilute, Cat: ZF-0511), Goat anti-mouse Alexa Fluor 594 (1:500 dilute, Cat: ZF-0513), Secondary goat anti-rabbit IgG-HRP antibody (1:2500 dilute, Cat: ZF-0516) and Goat anti-mouse IgG-HRP antibody (1:2500 dilute, Cat: ZF-0512) were purchased from Beijing Zhong Shan -Golden Bridge Biological Technology CO, LTD.

The reagents used included indole propionic acid (IPA) (≥ 99% pure, Cat:57400-5G-F, Sigma-Aldrich, MO, US), TCP (≥ 98% pure, CAS: 6515-38-4, Adamas, Shanghai, China), dihydroethidium (DHE) (Cat: D7008-10MG, Sigma-Aldrich, MO, US), corn oil (CAS:8001-30-7, Solarbio, Beijing, China). Test kits involved Hematoxylin-Eosin Staining (H&E) Kit (Cat: C0105S, Beyotime, Shanghai, China), ROS Assay Kit (Cat: S0033M, Beyotime, Shanghai, China), TUNNEL staining kit (Cat: C1088, Beyotime, Shanghai, China) and FasKing One Step Rt-qPCR Kit (Cat: FP313-01, Tiangen, Beijing, China).

Animals and IPA treatment

All the animal procedures were approved by the Hangzhou Normal University Animal Welfare Ethics Committee (permit no. HSD20220601),and were carried out in accordance with the National Institutes of Health Guidelines for the Care and Use of Laboratory Animals(NIH Publication NO.85 – 23, revised 2011). The study was also carried out in compliance with the ARRIVE guidelines. To reduce the interfering effects of sex hormones and other factors on the auditory system, male C57BL/6 mice were used to test[45]. Mice were housed in an SPF-grade animal room at the Laboratory Animal Center of Hangzhou Normal University. All animals had free access to food and water. They were maintained in an environment with controlled temperature settings ranging from 22 ℃ to 24 ℃, a relative humidity of 60%, and a 12-hour light/dark cycle.

Healthy male C57BL/6 mice aged 6–8 weeks (Shanghai SLAC Laboratory Animal Co., Ltd., Shanghai, China) with a body weight of 18–25 g and normal hearing were selected as the experimental animals. Mice were randomly divided into five groups ($n = 10$ per treatment condition) and treated as follows: (1) 10 ml/kg/d corn oil (control group); (2) 40 mg/kg/d IPA (40 mg/kg IPA group); (3) 50 mg/kg/d TCP (50 mg/kg TCP group); (4) 50 mg/kg/d TCP and 20 mg/kg/d IPA (20 mg/kg IPA + 50 mg/kg TCP group); and (5) 50 mg/kg/day TCP and 40 mg/kg/day IPA (40 mg/kg IPA + 50 mg/kg TCP group). Corn oil, TCP, or IPA were administered by gavage for 21 consecutive days. IPA (20 and 40 mg/kg) and TCP (50 mg/kg) solutions were prepared daily. In this study, the dosages of TCP (50 mg/kg) and IPA (20 and 40 mg/kg) were selected according to previously published data[20,46,47]. The 40 mg/kg IPA group was set to investigate its ototoxic.

After the final auditory brainstem response (ABR) tests, the mice were anesthetized via intraperitoneal injection of 5% pentobarbital sodium and subsequently decapitated. The right and left temporal bones of mice were dissected as a whole, respectively. Bilateral auditory vesicles were rapidly removed, and the cochlear tissue was collected and detached. One cochlea was fixed and preserved in 4% paraformaldehyde (PFA), and the other cochlea was quickly frozen in liquid nitrogen and preserved at -80 °C for subsequent experiments.

Functional evaluation by ABR

ABR measurements were performed seven days before the start of the experiment to screen mice with normal hearing and 21 days after treatment. Before the ABR test, mice were anesthetized by intraperitoneal injection of 5% pentobarbital sodium During the auditory brainstem response (ABR) tests, the body temperature of the experimental mice was maintained at 37 ± 1 °C. The ABR test was conducted in a standard soundproof room using brain waves (Click) (90 – 10 dB SPL in -10 dB steps) and pure tones (Tone) at 8, 16, and 32 Hz (90 – 10 Db SPL in -10 dB steps) with 1,024 repetitions. Stimuli were transmitted via headphones and recording electrodes were placed subcutaneously at the median cranial apex of the mouse, with reference electrodes placed at the ipsilateral mastoid and grounded at the root of the nose to record electrophysiological responses. The stimulus intensity ranged from 90 to 10 dB SPL, beginning at 90 dB and decreasing every 10 dB until the disappearance of characteristic wave II, and the sound intensity at which this wave was no longer detected was recorded as the ABR threshold. Finally, graphs were plotted according to the stimulus level (dB sound pressure level [SPL]).

Immunofluorescence on cryosections

After dissection, the cochlea was immersed in 4% paraformaldehyde (PFA) for overnight fixation and subsequently decalcified in 0.5 M sodium ethylenediaminetetraacetic acid (EDTA) at 4°Cfor 5~7 days. The cochlear basement membrane was then separated using a dissection microscope. The specimen was then blocked and permeabilized with blocking buffer (10% horse serum and 0.03% saponin dissolved in 0.1% Triton X-100, PBS, pH = 7.4) for 1 h at room temperature. The specimens were immunolabelled with primary antibodies dissolved in PBST (3% horse serum, 0.1% Triton X-100,3% BSA, PBS, pH 7.4) overnight at 4 °C. The following primary antibodies were used: rabbit anti-Myosin7a (1:1000) for labeling HCs and mouse anti- III Tubulin β (1:500) for labeling SGNs. Next, specimens were incubated with goat anti-rabbit Alexa Fluor 488 (1:500) and goat anti-mouse Alexa Fluor 594 (1:500), dissolved in PBST (0.2% Triton X-100,1% BSA, pH 7.4) at 4 °C overnight. After washing with PBS, re-staining was performed in an anti-quenching sealer containing DAPI (Cat: ab104139-20, Abcam, Cambridges, UK) and placed on slides. All images were acquired using a Zeiss microscope (Jena, Germany) at the same settings. To quantify the HC data, 40×low-magnification images were randomly acquired. The number of HCs was counted and the results were averaged for each trial image with the staining results presented as 50 μm.

Hematoxylin-eosin staining of cryosections

The cochlear cryosections were dried in an electronic oven at 55 °C for 2 h. After decalcification, washing, and dehydration, samples were embedded in paraffin wax. Hematoxylin-eosin (HE) staining of cochlear cryosections was carried out using the Beyotime Hematoxylin-Eosin Staining Kit. The stained sections were mounted with neutral gum and examined under a light microscope. Each cochlea sample was assessed for the structure and arrangement of HCs, morphology and quantity of SGNs within the organ of Corti, and morphology of the SV and SL. In addition, the number of SGNs and thickness of the SV were counted and plotted for each group.

Immunofluorescence on cryosections

Cochlear samples were extracted from the dissected mice and subsequently fixed in 4% paraformaldehyde at 4 °C for 24 h. The cochlea was then decalcified, dehydrated, and embedded in OCT gel (CAS: 4583, Cherry Blossom, United States). The samples were then stored at -80 °C. The cochlear tissue cryosections were cut into 12 μm slices using cryosections. Subsequently, the cochlear cryosections were placed in an electronic oven at 55 °C for 2 h to dry. Subsequently, the sections were washed, blocked, and permeabilized as previously described. Sections were treated with rat anti-Ly6G (1:500) dissolved in PBST (3% horse serum, 0.1% Triton X-100,3% BSA, PBS, pH 7.4) and incubated overnight at 4 °C. After washing with PBS, the sections were incubated with secondary antibody for 2 h at room temperature. Secondary antibodies included goat anti-rabbit Alexa Fluor 488 (1:500) and goat anti-mouse Alexa Fluor 594 (1:500). All images were captured using a fluorescence microscope (Nikon, Japan) and a Zeiss microscope (Jena, Germany), both with identical settings.

Dihydroethidium (DHE) staining

DHE is a cell membrane-permeable blue probe that reacts with superoxide anions upon entry into the cell to form 2-hydroxy ethidium, which is used to assess the amount of ROS in the cochlea. 2-hydroxy ethidium produces red fluorescence when inserted into nucleic acids and can be detected by fluorescence microscopy. Briefly, cochlear slices were incubated with 1 μM DHE solution and then incubated for 60 min at 37 °C in dark.

After rinsing with PBS three times, a drop of mounting medium containing DAPI (for nuclei) was added to the sections. Finally, the section was covered with a coverslip and the edges were sealed with clear nail polish. In all immunofluorescence analyses, the fluorescence signals were measured semi-quantitatively: the fluorescence intensity of each area of interest corresponded to SGNs, HCs, and SV, respectively.

TUNEL staining

Apoptosis in SGN and HCs was assessed using a TUNEL staining kit. Sections of cochlear tissue embedded in paraffin were prepared, and paraffin was subsequently removed using xylene, followed by a series of ethanol treatments. After washing with PBS, the samples were incubated with a TUNEL reaction mixture (Roche, Switzerland) at 37 °C for 60 min and then stained with DAPI to label the nuclei. Three random microscopic fields per slide were examined under a fluorescence microscope (Nikon, Japan) and a Zeiss microscope (Jena, Germany).

RNA sequencing

We performed RNA-seq to explore changes in gene expression in the cochlea after IPA and TCP exposure. Cochlear samples were collected from mice that had undergone 21 days of IPA (20 mg/kg per day or 40 mg/kg per day), PBS-treated controls, or simultaneous treatment with TCP (50 mg/mL). Each group was divided into three biological replicates. RNA was extracted using an RNeasy Kits (Qiagen). RNase-free DNase I (Qiagen) was added to remove residual DNA and the mixture was incubated at 23 °C. The RNA concentration and purity were assessed using a NanoDrop Bioanalyzer. Construction of cDNA libraries was carried out at the Imperial BRC Genomics Facility using the TruSeq Sample Preparation Kit A (Illumina), followed by sequencing with the Illumina Novaseq 6000 (PE150) system. Differentially expressed genes (DEGs) were selected using edgeR software according to the threshold of Padj < 0.05 and |log2FC| > 1. GO analysis was performed on the DEGs. To identify IPA-dependent specific DEGs, the IPA-TCP vs. TCP and IPA vs. Ctrl groups were analyzed to identify the uniquely up-regulated or down-regulated genes.

Statistical analysis

All data are presented as mean ± SD. One-way ANOVA followed by Bonferroni post hoc test was used for multiple-group comparisons. Statistical analyses were performed using SPSS 24.0 (IBM, NY, USA) and GraphPad Prism 8 (GraphPad, CA, USA). A *p*-value of less than 0.05 was deemed statistically significant.

Data availability

The data that support the findings of this study are openly available in National Genomics Data Center, China National Center for Bioinformation Beijing Institute of Genomics, Chinese Academy of Sciences at https://bigd.big.ac.cn/gsa, reference number CRA019115.

Received: 9 November 2024; Accepted: 14 February 2025
Published online: 19 March 2025

References

1. McMahon, C. M., Nieman, C. L., Thorne, P. R., Emmett, S. D. & Bhutta, M. F. The inaugural World Report on hearing: from barriers to a platform for change. *Clin. Otolaryngol.* **46**, 459–463 (2021).
2. Gu, X. et al. Identification of common stria vascularis cellular alteration in sensorineural hearing loss based on ScRNA-seq. *BMC Genom.* **25**, 213 (2024).
3. Makary, C. A., Shin, J., Kujawa, S. G., Liberman, M. C. & Merchant, S. N. Age-related primary cochlear neuronal degeneration in human temporal bones. *J. Assoc. Res. Otolaryngol.* **12**, 711–717 (2011).
4. Cunningham, L. L. & Tucci, D. L. Hearing loss in adults. *N Engl. J. Med.* **377**, 2465–2473 (2017).
5. Freyer, D. R. et al. Prevention of cisplatin-induced ototoxicity in children and adolescents with cancer: a clinical practice guideline. *Lancet Child. Adolesc. Health*. **4**, 141–150 (2020).
6. Lopez-Poveda, E. A. et al. Predictors of hearing-aid outcomes. *Trends Hear.* **21**, 2331216517730526 (2017).
7. Li, K., Zhou, R., Zheng, W., Zhang, Y. & Qiu, J. Knowledge, attitude, and practice toward cochlear implants among deaf patients who received cochlear implants. *Sci. Rep.* **14**, 4451 (2024).
8. Zhang, L. et al. AAV-mediated gene cocktails enhance supporting cell reprogramming and hair cell regeneration. *Adv. Sci. (Weinheim Ger)*. **11**, e2304551 (2024).
9. Atkinson, P. J., Wise, A. K., Flynn, B. O., Nayagam, B. A. & Richardson, R. T. Viability of long-term gene therapy in the cochlea. *Sci. Rep.* **4**, 4733 (2014).
10. Xu, W. et al. Natural products: protective effects against sensorineural hearing loss. *Phytochem Rev.* **4**, 1–27 (2024).
11. Gao, J. et al. Impact of the gut microbiota on intestinal immunity mediated by Tryptophan Metabolism. *Front. Cell. Infect. Microbiol.* **8**, 13 (2018).
12. Lin, J., Sun-Waterhouse, D. & Cui, C. The therapeutic potential of diet on immune-related diseases: based on the regulation on tryptophan metabolism. *Crit. Rev. Food Sci. Nutr.* **62**, 8793–8811 (2022).
13. Dodd, D. et al. A gut bacterial pathway metabolizes aromatic amino acids into nine circulating metabolites. *Nat. (London U K)*. **551**, 648–652 (2017).
14. Niu, B. et al. The therapeutic potential of dietary intervention: based on the mechanism of a tryptophan derivative-indole propionic acid on metabolic disorders. *Crit. Rev. Food Sci. Nutr.* **8**, 1–20 (2024).
15. Feng, Y. et al. PXR activation relieves Deoxynivalenol-Induced Liver oxidative stress Via Malat1 LncRNA m(6)a demethylation. *Adv. Sci. (Weinheim Ger)*. **11**, e2308742 (2024).
16. Serger, E. et al. The gut metabolite indole-3 propionate promotes nerve regeneration and repair. *Nat. (London U K)*. **607**, 585–592 (2022).
17. Garcez, M. L., Tan, V. X., Heng, B. & Guillemin, G. J. Sodium Butyrate and Indole-3-propionic acid prevent the increase of cytokines and Kynurenine Levels in LPS-induced human primary astrocytes. *Int. J. Tryptophan Res.* **13**, 1178646920978404 (2020).
18. Yisireyili, M., Takeshita, K., Saito, S., Murohara, T. & Niwa, T. Indole-3-propionic acid suppresses indoxyl sulfate-induced expression of fibrotic and inflammatory genes in proximal tubular cells. *Nagoya J. Med. Sci.* **79**, 477–486 (2017).

19. Karbownik, M., Garcia, J. J., Lewiński, A. & Reiter, R. J. Carcinogen-induced, free radical-mediated reduction in microsomal membrane fluidity: reversal by indole-3-propionic acid. *J. Bioenerg Biomembr.* **33**, 73–78 (2001).
20. Owumi, S. E., Adedara, I. A. & Oyelere, A. K. Indole-3-propionic acid mitigates chlorpyrifos-mediated neurotoxicity by modulating cholinergic and redox-regulatory systems, inflammatory stress, apoptotic responses and DNA damage in rats. *Environ. Toxicol. Pharmacol.* **89**, 103786 (2022).
21. Huang, M. et al. 3,5,6-Trichloro-2-pyridinol confirms ototoxicity in mouse cochlear organotypic cultures and induces cytotoxicity in HEI-OC1 cells. *Toxicol. Appl. Pharmacol.* **475**, 116612 (2023).
22. Huang, M. et al. Pesticide metabolite 3, 5, 6-trichloro-2-pyridinol causes massive damage to the cochlea resulting in hearing loss in adult mice. *Environ. Pollut (Oxford U K)*. **360**, 124691 (2024).
23. Zou, M., Huang, M., Zhang, J. & Chen, R. Exploring the effects and mechanisms of organophosphorus pesticide exposure and hearing loss. *Front. Public. Health*. **10**, 1001760 (2022).
24. Kalinec, G., Thein, P., Park, C. & Kalinec, F. HEI-OC1 cells as a model for investigating drug cytotoxicity. *Hear. Res.* **335**, 105–117 (2016).
25. Yang, Z., Min, Z. & Yu, B. Reactive oxygen species and immune regulation. *Int. Rev. Immunol.* **39**, 292–298 (2020).
26. Sas, A. R. et al. A new neutrophil subset promotes CNS neuron survival and axon regeneration. *Nat. Immunol.* **21**, 1496–1505 (2020).
27. Konopelski, P. & Mogilnicka, I. Biological Effects of Indole-3-Propionic Acid, a Gut Microbiota-Derived Metabolite, and Its Precursor Tryptophan in Mammals' Health and Disease. *Int. J. Mol. Sci.* **23**, 1222 (2022).
28. Min, X. et al. BDNF-enriched small extracellular vesicles protect against noise-induced hearing loss in mice. *J. Controlled Release*. **364**, 546–561 (2023).
29. Benito-Orejas, J. I., Ramírez, B., Morais, D., Almaraz, A. & Fernández-Calvo, J. L. Comparison of two-step transient evoked otoacoustic emissions (TEOAE) and automated auditory brainstem response (AABR) for universal newborn hearing screening programs. *Int. J. Pediatr. Otorhinolaryngol.* **72**, 1193–1201 (2008).
30. Zhang, L. et al. 4-octyl itaconate alleviates cisplatin-induced ferroptosis possibly via activating the NRF2/HO-1 signalling pathway. *J. Cell. Mol. Med.* **28**, e18207 (2024).
31. Zhang, H. et al. Natural Multifunctional Silk Microcarriers for noise-Induced hearing loss therapy. *Adv. Sci. (Weinheim Ger)*. **11**, e2305215 (2024).
32. Fetoni, A. R., Paciello, F., Rolesi, R., Paludetti, G. & Troiani, D. Targeting dysregulation of redox homeostasis in noise-induced hearing loss: oxidative stress and ROS signaling. *Free Liberal Biol. Med.* **135**, 46–59 (2019).
33. Pizzino, G. et al. Oxidative Stress: Harms and Benefits for Human Health. *Oxid. Med. Cell. Longevity* 8416763 (2017).
34. Bousquet, P. A. et al. Abstract 1782: Reactive oxygen species (ROS) and mitochondrial DNA (mtDNA) damage in tumor hypoxia, poor radiotherapy response, and metastatic progression of rectal cancer. *Cancer Res.* 77, 1782, (2017).
35. Li, N. et al. Curcumin protects against the age-related hearing loss by attenuating apoptosis and senescence via activating Nrf2 signaling in cochlear hair cells. *Biochem. Pharmacol. (Amsterdam Neth)*. **212**, 115575 (2023).
36. Kara, M. et al. Evaluation of the protective effects of hesperetin against cisplatin-induced ototoxicity in a rat animal model. *Int. J. Pediatr. Otorhinolaryngol.* **85**, 12–18 (2016).
37. Wang, S. et al. Electroconductive and Immunomodulatory Natural polymer-based hydrogel bandages designed for peripheral nerve regeneration. *Adv. Funct. Mater.* **34**, 2310903 (2024).
38. Korbecki, J., Barczak, K., Gutowska, I., Chlubek, D. & Baranowska-Bosiacka, I. CXCL1: Gene, promoter, regulation of expression, mRNA Stability, Regulation of activity in the Intercellular Space. *Int. J. Mol. Sci.* **23**, 792 (2022).
39. Kui, L., Kim, A. D., Onyuru, J., Hoffman, H. M. & Feldstein, A. E. BRP39 regulates Neutrophil Recruitment in NLRP3 Inflammasome-Induced Liver inflammation. *Cell. Mol. Gastroenterol. Hepatol.* **17**, 481–497 (2024).
40. Stoler, I. et al. Gene-dose effect of MEFV Gain-of-function mutations determines ex vivo neutrophil activation in familial Mediterranean Fever. *Front. Immunol.* **11**, 716 (2020).
41. He, L. et al. The immunomodulatory role of matrix metalloproteinases in colitis-associated cancer. *Front. Immunol.* **13**, 1093990 (2022).
42. Selders, G. S., Fetz, A. E., Radic, M. Z. & Bowlin, G. L. An overview of the role of neutrophils in innate immunity, inflammation and host-biomaterial integration. *Regener Biomater.* **4**, 55–68 (2017).
43. Warre-Cornish, K. et al. Interferon-γ signaling in human iPSC-derived neurons recapitulates neurodevelopmental disorder phenotypes. *Adv. Sci.* **6**, eaay9506 (2020).
44. Wang, X. et al. Driving axon regeneration by orchestrating neuronal and non-neuronal innate immune responses via the IFNγ-cGAS-STING axis. *Neuron* **111**, 236–255e237 (2023).
45. Lin, N., Urata, S., Cook, R. & Makishima, T. Sex differences in the auditory functions of rodents. *Hear. Res.* **419**, 108271 (2022).
46. Hanley, T. R. Jr., Carney, E. W. & Johnson, E. M. Developmental toxicity studies in rats and rabbits with 3,5,6-trichloro-2-pyridinol, the major metabolite of chlorpyrifos. *Toxicol. Sci.* **53**, 100–108 (2000).
47. Deng, Y., Zhang, Y., Lu, Y., Zhao, Y. & Ren, H. Hepatotoxicity and nephrotoxicity induced by the chlorpyrifos and chlorpyrifos-methyl metabolite, 3,5,6-trichloro-2-pyridinol, in orally exposed mice. *Sci. Total Environ.* **544**, 507–514 (2016).

Acknowledgements

This research was supported by Zhejiang Provincial Natural Science Foundation of China under Grant number LTGD24C040002; and Hangzhou special support programs for high-level talents in 2021.

Author contributions

Shuangshuang Mao: Data curation, Investigation, Validation. Zirui Zhang: Data curation, Writing – original draft. Mao Huang: Data curation, Formal analysis, Investigation. Ziying Zhang Investigation, Methodology. Yu Hong : Writing – original draft. Xiaohua Tan: Supervision. Fei Gui: Funding acquisition, Validation. Yifei Cao: Funding acquisition, Writing – original draft. Fuzhi Lian: Conceptualization, Writing – review & editing. Rong Chen: Funding acquisition, Supervision, Writing – review & editing.

Declarations

Competing interests

The authors declare no competing interests.

Additional information

Supplementary Information The online version contains supplementary material available at https://doi.org/10.1038/s41598-025-90655-3.

Correspondence and requests for materials should be addressed to Y.C., F.L. or R.C.